Acta Crystallographica Section F
Structural Biology and Crystallization Communications
ISSN 1744-3091

Expression, purification, crystallization and preliminary crystallographic analysis of PilA from the nontypeable *Haemophilus influenzae* type IV pilus

Subramaniapillai Kolappan,[a] Erin N. Tracy,[b] Lauren O. Bakaletz,[b] Robert S. Munson Jr[b] and Lisa Craig[a]*

[a]Molecular Biology and Biochemistry Department, Simon Fraser University, Burnaby, BC V5A 1S6, Canada, and [b]Center for Microbial Pathogenesis, The Research Institute at Nationwide Children's Hospital and The Center for Microbial Interface Biology, The Ohio State University, Columbus, OH 43205, USA

Correspondence e-mail: licraig@sfu.ca

Received 19 September 2011
Accepted 23 October 2011

The type IV pili of nontypeable *Haemophilus influenzae* (NTHi) are involved in twitching motility, adherence, competence and biofilm formation. They are potential virulence factors for this important human pathogen and are thus considered to be vaccine targets. To characterize these pili, an attempt to solve the atomic structure of the major pilin subunit PilA was initiated. A 1.73 Å resolution X-ray diffraction data set was collected from native N-terminally truncated PilA (ΔN-PilA). Data processing indicated a hexagonal crystal system, which was determined to belong to space group $P6_1$ or $P6_5$ based on the systematic absences and near-perfect twinning of the crystal. The unit-cell parameters were $a = b = 68.08$, $c = 197.03$ Å with four molecules in the asymmetric unit, giving a solvent content of 50%. Attempts to solve the ΔN-PilA structure by molecular replacement with existing type IV pilin and type II secretion pseudopilin structures are in progress.

1. Introduction

Nontypeable *Haemophilus influenzae* (NTHi) are opportunistic Gram-negative bacterial pathogens that infect both the upper and the lower respiratory tracts (Murphy, 2003). These unencapsulated strains of *H. influenzae* cause numerous illnesses, including sinusitis, recurrent otitis media and exacerbations of chronic obstructive pulmonary disease and bronchitis. NTHi express type IV pili (T4P), hairlike filaments with diverse functions critical to pathogenesis in many Gram-negative bacteria (Ayers *et al.*, 2010; Craig & Li, 2008; Pelicic, 2008). In NTHi, T4P are involved in adherence, twitching motility and biofilm formation (Bakaletz *et al.*, 2005; Jurcisek & Bakaletz, 2007; Jurcisek *et al.*, 2007).

Type IV pili are only 60–90 Å in diameter and 1 µm or more in length and are comprised of thousands of copies of the major pilin protein. Crystal structures of full-length type IV pilins revealed an extended N-terminal α-helix and a globular C-terminal domain with a central β-sheet and a C-terminal disulfide bridge delineating the D-region (Craig *et al.*, 2003, 2006; Parge *et al.*, 1995; Hartung *et al.*, 2011). The highly conserved N-terminal α-helix serves as the polymerization domain and the variable C-terminal globular domain forms the pilus surface and defines many of its diverse functions (Craig & Li, 2008). The NTHi pilin subunit PilA is a member of the type IVa pilin subclass, which differ from the type IVb pilins in the lengths of the signal peptide, D-region and mature protein as well as in the topology of the globular domain (Craig & Li, 2008). In addition to the conserved C-terminal cysteine pair, NTHi PilA has two central cysteines, similar to PilA from *Pseudomonas aeruginosa* strain K122-4 and FimA from *Dichelobacter nodosus*. The PilA sequence is relatively conserved in NTHi disease isolates, with the exception of a short segment flanking one of the central cysteines and another segment towards the C-terminus of the protein. Thus, these pili are attractive targets for broad-specificity NTHi vaccines (Novotny *et al.*, 2009, 2011). The atomic structure of the NTHi type IV pilin would be of great value in the design of vaccine candidates and may provide insights into the role of these pili in pathogenesis. Here, we describe our progress in determining the X-ray crystal structure of NTHi PilA.

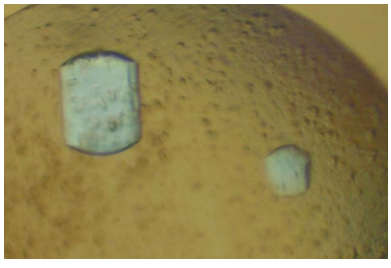

2. Materials and methods

2.1. Expression and purification of ΔN-PilA

The *pilA* gene fragment encoding residues 29–137 (ΔN-PilA) was PCR-amplified from NTHi strain 86-028NP genomic DNA (Bakaletz *et al.*, 2005; Jurcisek & Bakaletz, 2007; Jurcisek *et al.*, 2007) using the primer GCG**CATATG**ACTAAAAAAGCAGCGGTATCTG containing an *Nde*I site and the primer GCC**AGATCT**GCCATTTTGAGCGGTTACAC containing a *Bgl*II site. The *pilA* gene fragment was cloned into the pET15b vector (Novagen), which encodes an N-terminal hexahistidine tag (His tag) and linker, as described by Carruthers *et al.* (work submitted). A plasmid with the correct sequence was designated pRSPILA. *Escherichia coli* Origami (DE3) cells (Novagen) transformed with pRSPILA were grown in 6 l Luria broth containing ampicillin (100 µg ml^{-1}) and kanamycin (30 µg ml^{-1}) with shaking at 310 K until they reached an OD_{600} of ∼0.4. At this point, isopropyl β-D-1-thiogalactopyranoside was added to a final concentration of 0.4 m*M* to induce ΔN-PilA expression and the cells were grown for a further 18 h at 292 K. All purification steps were carried out at 277 K. The cells were harvested by centrifugation at 5000*g* for 30 min and then flash-cooled in liquid nitrogen and thawed to disrupt the cell membranes. The cell pellets were resuspended in lysis buffer (50 m*M* Na_2HPO_4/NaH_2PO_4 pH 7.4, 500 m*M* NaCl) with 1 mg ml^{-1} lysozyme and protease-inhibitor cocktail (EDTA-free, Roche Pharmaceuticals) and incubated for 1 h at room temperature. The cells were lysed by sonication and centrifuged at 40 000*g* for 1 h to remove cell debris. The supernatant was loaded onto an Ni–NTA column (GE Healthcare) pre-equilibrated with lysis buffer and 40 m*M* imidazole pH 7.4. The column was washed with the same buffer and the protein was eluted using 300 m*M* imidazole. The protein was concentrated using an Amicon stirred-cell concentrator (Millipore) and loaded onto a Sephacryl S-100 size-exclusion column pre-equilibrated with 20 m*M* Tris–HCl pH 7.4, 50 m*M* NaCl, 1 m*M* EDTA. Peak fractions were pooled together and concentrated to 20 mg ml^{-1} using a stirred-cell concentrator. The ΔN-PilA protein was greater than 95% pure as assessed by a Coomassie-stained SDS–PAGE gel. Its identity was confirmed by mass spectrometry (data not shown).

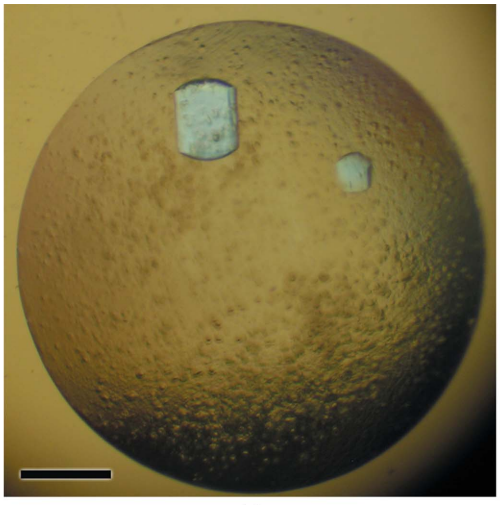

(*a*)

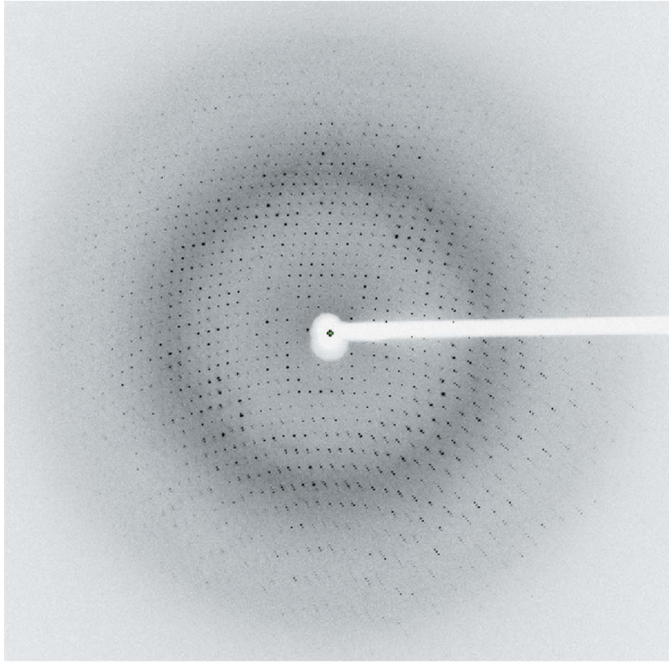

(*b*)

Figure 1
ΔN-PilA crystals and X-ray diffraction. (*a*) *H. influenzae* ΔN-PilA crystal after seven months of growth in 20 m*M* Tris–HCl pH 7.4, 200 m*M* $LiSO_4$, 1 *M* potassium/sodium tartrate. (*b*) Representative diffraction image for the ΔN-PilA crystal displayed in the program *MOSFLM* (Leslie, 1992). The resolution at the edge of the image is 1.7 Å.

2.2. Crystallization

ΔN-PilA crystals were obtained using the hanging-drop vapour-diffusion method with 2 µl protein solution (20 mg ml^{-1}) and 2 µl reservoir solution. Diffraction-quality crystals of ΔN-PilA grew in 20 m*M* Tris–HCl pH 7.4, 200 m*M* $LiSO_4$, 1 *M* potassium/sodium tartrate (Fig. 1*a*) after approximately seven months at 293 K. The crystals were cryoprotected using glycerol by first transferring them into mother liquor with 5%(*v*/*v*) glycerol and then increasing the glycerol content incrementally by 5% to a final concentration of 25% prior to freezing and storage in liquid nitrogen.

2.3. Diffraction data collection and processing

A native ΔN-PilA data set was collected on beamline 08ID-1 (CMCF-ID) at the Canadian Light Source (CLS; Fig. 1*b*). Raw diffraction data were reduced using *XDS* (Kabsch, 2010) and scaled to 1.73 Å resolution using *XSCALE*. The data quality was assessed using *SFCHECK* (Vaguine *et al.*, 1999) and the solvent content was calculated using *MATTHEWS_COEF* from *CCP*4 (Winn *et al.*, 2011). The programs *Phaser* (McCoy *et al.*, 2007), *MOLREP* (Vagin & Teplyakov, 2010), *EPMR* (Kissinger *et al.*, 1999; Long *et al.*, 2008) and *BALBES* (Long *et al.*, 2008) were used for molecular-replacement trials, with the type IVa pilins from *Neisseria gonorrhoeae* (PilE; PDB entry 2hi2; Craig *et al.*, 2006), *Pseudomonas aeruginosa* (PilA, PDB entry 1oqw, Craig *et al.*, 2003; K122-4 pilin, PDB entry 1qve, Audette *et al.*, 2004; Pa110594 pilin, PDB entry 3jyz, Nguyen *et al.*, 2010), *Dichelobacter nodosus* (FimA; PDB entry 3sok; Hartung *et al.*, 2011) and *Francisella tularensis* (PilA; PDB entry 3soj; Hartung *et al.*, 2011) as well as the type II secretion pseudopilin PulG from *Klebsiella oxytoca* (PDB entry 1t92; Köhler *et al.*, 2004) as search models.

3. Results and discussion

Recombinant ΔN-PilA was expressed in *E. coli* Origami cells at high levels, resulting in a yield of 5 mg purified protein per litre of cell culture at ∼95% purity. The crystals took many months to grow and resulted in only a few diffraction-quality crystals, from which a single

1.73 Å resolution data set was collected. The native ΔN-PilA data set was initially processed using *XDS*, which suggested a hexagonal crystal system (quality of fit 2.2 for primitive hexagonal). The unit-cell parameters were $a = b = 68.08$, $c = 197.03$ Å, $\alpha = \beta = 90$, $\gamma = 120^\circ$ (Table 1). The processed data scaled well in 622, the highest symmetry in the hexagonal system, and *XSCALE* gave an $R_{\rm merge}$ of 5.9% overall (41.6% for the highest resolution shell, 1.90–1.73 Å) and an $\langle I/\sigma(I)\rangle$ of 10.2 (2.2 for the highest resolution shell). Upon manual inspection of the reflection file, only the $l = 6n$ reflections were present for 00l, thereby identifying a $6_1/6_5$ screw and suggesting that the ΔN-PilA crystal belonged to either space group $P6_122$ or $P6_522$. A twin test was performed on the data set using the *Merohedral Twin Detector: Padilla–Yeates Algorithm* (http://nihserver.mbi.ucla.edu/pystats/; Padilla & Yeates, 2003), which gave $\langle|L|\rangle$ and $\langle L^2\rangle$ of 0.344 and 0.171 (Fig. 2), respectively, consistent with close-to-perfect twinning ($\langle|L|\rangle = 0.500$ and $\langle L^2\rangle = 0.333$ for untwinned crystals and $\langle|L|\rangle = 0.375$ and $\langle L^2\rangle = 0.200$ for perfectly twinned crystals). The data set was further evaluated with *CTRUNCATE* in *CCP*4 (Winn *et al.*, 2011), which confirmed near-perfect twinning. Since twinning is not possible for the 622 point group (Yeates, 1997) and the systematic absences ruled out all space groups in the *P*312 and *P*321 crystal systems, the space group was assigned as $P6_1$ or its enantiomorph $P6_5$. For a solvent content of ∼50%, there are four ΔN-PilA molecules in the asymmetric unit based on the Matthews coefficient calculation (Matthews, 1968).

We are currently attempting to solve the ΔN-PilA structure by molecular replacement with type IV pilins of known structure using data scaled in $P6_1/P6_5$ as well as other possible trigonal and hexagonal space groups. NTHi is most similar in sequence to the type IV pilin PilE from *N. gonorrhoeae* (46% amino-acid sequence identity for the first 86 residues) and PAK pilin (44% identity) and K122-4 pilin (41% identity) from *P. aeruginosa*. However, sequence similarity is strongest in the N-terminal ∼25 amino acids of these pilins, which are absent in ΔN-PilA. All available type IVa pilin structures and also the type II secretion pseudopilin PulG were used as search models. Side chains were removed and replaced by alanines (polyalanine models) or by glycines (polyglycine models) in *Coot* (Emsley & Cowtan, 2004). Polyalanine/polyserine models were also generated in which a hydroxyl was added to C^β of residues with large side chains. In addition, a composite model generated in *Coot* from an overlay of all available type IVa pilin structures was used in molecular-replacement trials. Loops were removed from the models and the protruding segment of the N-terminal α-helix α1N was removed from full-length pilin structures. Thus far, none of the searches have yielded a structure solution. We are also attempting *ab initio* structure determination using the *ARCIMBOLDO* set of programs (Rodríguez *et al.*, 2009).

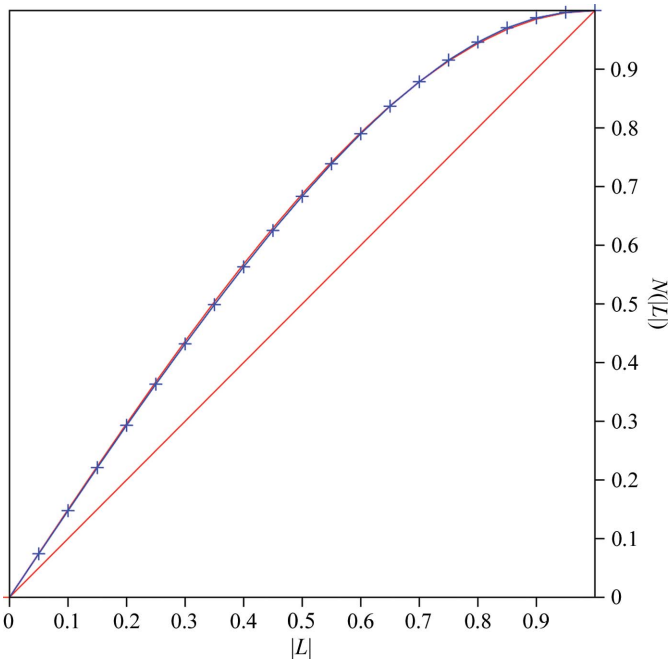

Figure 2
Twinning analysis. Results of analysis of ΔN-PilA ($P6_1/P6_5$) crystallographic data using the *Merohedral Twin Detector: Padilla–Yeates Algorithm* (http://nihserver.mbi.ucla.edu/pystats/). The red line represents theoretical untwinned data and the red curve represents theoretical perfectly twinned data. The blue curve is the observed data.

Table 1
Crystallographic data-collection statistics for ΔN-PilA.

Values in parentheses are for the highest resolution shell.

Beamline	CLS 08ID-1
Wavelength (Å)	1.0
Temperature (K)	100
Space group	$P6_1/P6_5$
Unit-cell parameters (Å, °)	$a = b = 68.08$, $c = 197.03$, $\alpha = \beta = 90.0$, $\gamma = 120.0$
Resolution (Å)	20.0–1.73
Completeness (%)	92.2 (66.2)
Observed reflections	488919
Unique reflections	52990
$R_{\rm merge}$† (%)	6.4 (48.4)
$\langle I/\sigma(I)\rangle$	22.0 (4.4)
Multiplicity	9.2 (8.5)
Wilson B value (Å^2)	29.8
Mosaicity (°)	0.2

† $R_{\rm merge} = \sum_{hkl}\sum_i |I_i(hkl) - \langle I(hkl)\rangle| / \sum_{hkl}\sum_i I_i(hkl)$, where $I_i(hkl)$ is the intensity of an individual reflection and $\langle I(hkl)\rangle$ is the average intensity of that reflection.

4. Conclusions

We have purified and crystallized N-terminally truncated NTHi PilA and obtained a high-resolution data set. However, structure determination by molecular replacement was impeded because of crystal twinning and the large number of molecules in the asymmetric unit. Furthermore, the existing pilin structures may not be sufficiently similar to PilA to provide a molecular-replacement solution. The native data set is likely to be of sufficient quality to determine the ΔN-PilA crystal structure if phases can be obtained by *ab initio* or MAD methods. Though challenging, the PilA structure is sure to reveal unique structural features that may provide insights into its functions in NTHi colonization and pathogenesis as well as aid in the design of vaccine candidates based on this important virulence determinant.

We thank Benjamin Hon for protein expression and purification and the beamline staff at the Canadian Light Source. This work was supported by operating grant R01 DC007464 from the National Institutes of Health to RSM. LC was supported by a New Investigator Award from the Canadian Institutes of Health Research and a Scholar Award from the Michael Smith Foundation for Health Research.

References

Audette, G. F., Irvin, R. T. & Hazes, B. (2004). *Biochemistry*, **43**, 11427–11435.
Ayers, M., Howell, P. L. & Burrows, L. L. (2010). *Future Microbiol.* **5**, 1203–1218.

Bakaletz, L. O., Baker, B. D., Jurcisek, J. A., Harrison, A., Novotny, L. A., Bookwalter, J. E., Mungur, R. & Munson, R. S. (2005). *Infect. Immun.* **73**, 1635–1643.
Craig, L. & Li, J. (2008). *Curr. Opin. Struct. Biol.* **18**, 267–277.
Craig, L., Taylor, R. K., Pique, M. E., Adair, B. D., Arvai, A. S., Singh, M., Lloyd, S. J., Shin, D. S., Getzoff, E. D., Yeager, M., Forest, K. T. & Tainer, J. A. (2003). *Mol. Cell*, **11**, 1139–1150.
Craig, L., Volkmann, N., Arvai, A. S., Pique, M. E., Yeager, M., Egelman, E. H. & Tainer, J. A. (2006). *Mol. Cell*, **23**, 651–662.
Emsley, P. & Cowtan, K. (2004). *Acta Cryst.* D**60**, 2126–2132.
Hartung, S., Arvai, A. S., Wood, T., Kolappan, S., Shin, D. S., Craig, L. & Tainer, J. A. (2011). *J. Biol. Chem.*, doi:10.1074/jbc.M111.297242.
Jurcisek, J. A. & Bakaletz, L. O. (2007). *J. Bacteriol.* **189**, 3868–3875.
Jurcisek, J. A., Bookwalter, J. E., Baker, B. D., Fernandez, S., Novotny, L. A., Munson, R. S. & Bakaletz, L. O. (2007). *Mol. Microbiol.* **65**, 1288–1299.
Kabsch, W. (2010). *Acta Cryst.* D**66**, 125–132.
Kissinger, C. R., Gehlhaar, D. K. & Fogel, D. B. (1999). *Acta Cryst.* D**55**, 484–491.
Köhler, R., Schäfer, K., Müller, S., Vignon, G., Diederichs, K., Philippsen, A., Ringler, P., Pugsley, A. P., Engel, A. & Welte, W. (2004). *Mol. Microbiol.* **54**, 647–664.
Leslie, A. G. W. (1992). *Jnt CCP4/ESF–EACBM Newsl. Protein Crystallogr.* **26**.
Long, F., Vagin, A. A., Young, P. & Murshudov, G. N. (2008). *Acta Cryst.* D**64**, 125–132.
Matthews, B. W. (1968). *J. Mol. Biol.* **33**, 491–497.
McCoy, A. J., Grosse-Kunstleve, R. W., Adams, P. D., Winn, M. D., Storoni, L. C. & Read, R. J. (2007). *J. Appl. Cryst.* **40**, 658–674.
Murphy, T. F. (2003). *Curr. Opin. Infect. Dis.* **16**, 129–134.
Nguyen, Y., Jackson, S. G., Aidoo, F., Junop, M. & Burrows, L. L. (2010). *J. Mol. Biol.* **395**, 491–503.
Novotny, L. A., Adams, L. D., Kang, D. R., Wiet, G. J., Cai, X., Sethi, S., Murphy, T. F. & Bakaletz, L. O. (2009). *Vaccine*, **28**, 279–289.
Novotny, L. A., Clements, J. D. & Bakaletz, L. O. (2011). *Mucosal Immunol.* **4**, 456–467.
Padilla, J. E. & Yeates, T. O. (2003). *Acta Cryst.* D**59**, 1124–1130.
Parge, H. E., Forest, K. T., Hickey, M. J., Christensen, D. A., Getzoff, E. D. & Tainer, J. A. (1995). *Nature (London)*, **378**, 32–38.
Pelicic, V. (2008). *Mol. Microbiol.* **68**, 827–837.
Rodríguez, D. D., Grosse, C., Himmel, S., González, C., de Ilarduya, I. M., Becker, S., Sheldrick, G. M. & Usón, I. (2009). *Nature Methods*, **6**, 651–653.
Vagin, A. & Teplyakov, A. (2010). *Acta Cryst.* D**66**, 22–25.
Vaguine, A. A., Richelle, J. & Wodak, S. J. (1999). *Acta Cryst.* D**55**, 191–205.
Winn, M. D. *et al.* (2011). *Acta Cryst.* D**67**, 235–242.
Yeates, T. O. (1997). *Methods Enzymol.* **276**, 344–358.